

Determination of Diffusion Coefficients of Water in Cellulose Acetate Membranes

MICHAEL J. PALIN,* GERALD J. GITTENS,** and G. BRIAN PORTER,
*Department of Chemistry and Metallurgy, The Royal Military College of Science,
Shrivenham, Wiltshire, England*

Synopsis

The determination of the diffusion coefficient for water in various porosity cellulose acetate membranes by a gravimetric method, using a humidified carrier gas, is described. It was found to be impossible to obtain meaningful results for very porous membranes, although dense membranes gave limiting values of diffusion coefficient at high carrier gas velocities. This phenomenon is explained in terms of the dissipation of the heat of sorption by the forced convection provided by the carrier gas. The variation of diffusion coefficient with concentration of water in dense cellulose acetate is explained in terms of clustering of water molecules in the polymer at high concentration.

INTRODUCTION

A common method for the determination of diffusion coefficients in polymers utilizes a vacuum technique in which the sample, initially evacuated, is exposed to a controlled vapor pressure source on sorption and to a vacuum again on desorption.¹ We have used a carrier gas flow technique to study the interaction between water and cellulose acetate reverse osmosis membranes and have measured the effects of humidity, flow rate, membrane structure, and equilibrium concentration.

EXPERIMENTAL

Materials

The preparation and morphology of the cellulose acetate (39.8% acetyl) membranes used are described by Gittens et al.² The membranes were cast from acetone-formamide dope, allowing various evaporation times, then immersed in iced water (Table I). The membrane with shorter evaporation times showed a heterogeneous structure, the 30-sec evaporation membrane having a three-layer structure dominated by a porous lower layer. The 48-hr evaporation membranes were essentially dense homogeneous films.

* Present address: Fisons Ltd., Levington Research Station, Ipswich, Suffolk, England.

** Present address: Department of Ceramic Technology, North Staffordshire Polytechnic, College Road, Stoke-on-Trent ST4 2DE, England.

TABLE I
Membrane Details

Membrane reference	Evaporation time	Surface area, m ² /g	
		N ₂ sorption (-196°C)	H ₂ O sorption (30°C)
S172	<5 sec	77	81
S171	30 sec	126	125
S170	3 min	67	97
S173	48 hr	7	144
S174	48 hr	2	80 (60°C)

Further characterization of these membranes (using freeze-dried samples²) by nitrogen adsorption, in a modified form of the apparatus due to Lippens et al.,³ allowed B.E.T. surface areas to be calculated (Table I). These results verified the degrees of porosity observed by electron microscopy,² as will be shown later in the discussion.

Apparatus

The apparatus shown in Figure 1 allowed membrane samples to be exposed to a range of relative humidities ($R.H. = P/P_0 \times 100$) at different temperatures. The change in weight of the membrane, sorption, or desorption was detected by a recording electrobalance (C. I. Electronics Ltd., Mark 2B).

Weight changes of the order of 20 mg for a 100-mg sample could be followed with a precision of 0.01 mg. Oxygen-free nitrogen, dried by molecular sieves, was used for "zero" humidity. Freeze-dried membrane samples were equilibrated with dried nitrogen prior to exposure to water vapor.

The membrane samples for diffusion coefficient measurement were thermostatted at 60°C, the actual temperature being given by a 0.1°C mercury thermometer close to the sample. The saturator thermostat contained a number of Dreschel bottles, filled with distilled water and equipped with glass sinters. At the end of the series were two bottles containing glass wool to remove entrained water droplets from the carrier gas. The carrier gas became saturated with water vapor at the temperature of the bath. The efficiency of saturation was tested by dew point determination of the carrier gas prior to entering the sample vessel. At all combinations of temperature and flow rate, saturation was found to be complete.

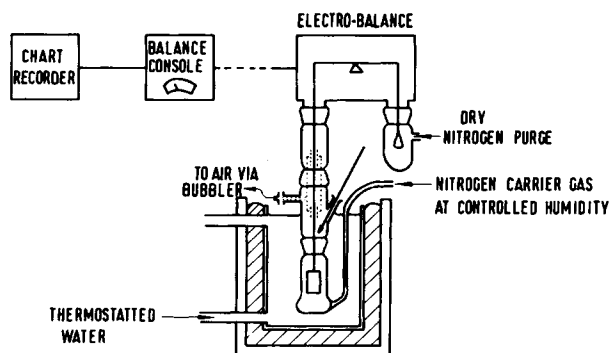


Fig. 1. Water sorption apparatus.

The maximum temperature required of the saturator bath was that of the sample, i.e., 100% R.H.; but in practice this temperature was never used, to avoid the possibility of condensation anywhere in the system. Various precautions to ensure that condensation and electrostatic effects did not influence the balance readings were taken. Heating tapes were wrapped around the saturator-to-sample vessel tube and around the sample vessel above the thermostat. A counterflow of dry nitrogen was blown across the balance head to exclude excess water vapor and to prevent thermomolecular streaming from the hotter region of the system. Adsorption of water vapor on to the thin, glass membrane suspension arm was avoided by coating it with silicone fluid before assembly. Electrostatic effects around the sample were neutralized by ionizing the gas with an α -source (Americium 244) and by earthing the brass baffle above the sample.

The flow of gas through the sample chamber was controlled using needle valves and monitored by flowmeters which had been calibrated against soap-bubble flowmeters. Other than the buoyancy effect on the sample, no disturbing effects of the gas flow were noted. Readings were taken with gas flowing.

Method and Calculation

For sorption kinetics, the dry sample was exposed to humidified carrier gas and its weight increase with time followed on a chart recorder. The equilibrium uptake, q_∞ , was taken at constant reading, usually at a time in excess of 2 hr. For desorption kinetics, the decrease in weight with time was recorded during exposure of the sample to dried carrier gas, again to a constant reading. The membrane thickness was measured at room humidity using a micrometer screw gauge.

Sorption by a plane sheet of membrane from an infinite reservoir, when the process is controlled by a diffusion coefficient (D), has been discussed by Crank and Park.^{1,4} For short times, the reduced form of the diffusion equation, eq. (1), may be used:

$$\frac{q_t}{q_\infty} = \frac{4}{l} (\bar{D} \cdot t / \Pi)^{1/2} \quad (1)$$

where q_t is the amount sorbed after time t , q_∞ is the uptake at infinite time (equilibrium sorption), l is the membrane thickness, and \bar{D} is the integral diffusion coefficient.

The experimental results consisted of pairs of values (q_t , t) obtained from the chart record using a digital reader. A computer program was used to provide plots of q_t/q_∞ against $4/l (t/\Pi)^{1/2}$ with slope $(\bar{D})^{1/2}$. These plots were found not to be linear over the whole sorption or desorption range, deviation depending on the total concentration change, being larger for larger changes. At short times, nonlinearity occurred because a finite time was required for the water vapor pressure in the sample vessel to reach its maximum experimental value. At large times, the diffusion coefficient becomes dependent on membrane water concentration causing a decrease in slope as saturation is approached.

If the diffusion coefficient is independent of the concentration, the sorption and desorption values, \bar{D}_A and \bar{D}_D , respectively, will be the same. Our results have shown, however, that the two are not the same, and it has been necessary to use eq. (2):

$$\bar{D} = 1/2(\bar{D}_A + \bar{D}_D). \quad (2)$$

This equation has been extensively used as a good approximation for the integral diffusion coefficient.¹

The diffusion coefficient and integral diffusion coefficient are equal, provided the diffusion coefficient is independent of concentration. If, however, a dependency exists they may be related by eq. (3)⁴:

$$D = \bar{D} \left(1 + C \cdot \frac{d \ln \bar{D}}{dC} \right) \quad (3)$$

RESULTS AND DISCUSSION

Sorption and desorption measurements were carried out on the dense, homogeneous membranes S173 and S174 and the more porous, heterogeneous membrane S171 at 60°C and 20% and 60% R.H., at various flow rates of the carrier gas. The results are plotted in Figures 2, 3, 4, 5, and 6. A further series of experiments was conducted on the dense film S174 to determine the dependence of diffusion coefficient on concentration (Fig. 10).

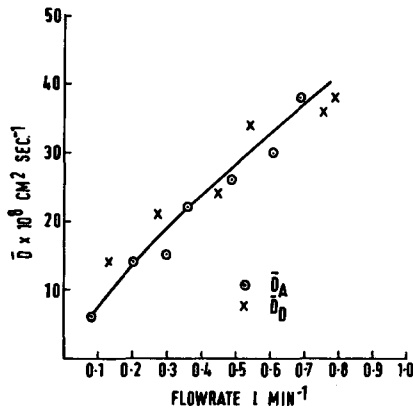


Fig. 2. Variation of \bar{D}_A and \bar{D}_D with flow rate of carrier gas at 60°C, 20% R.H. for S171.

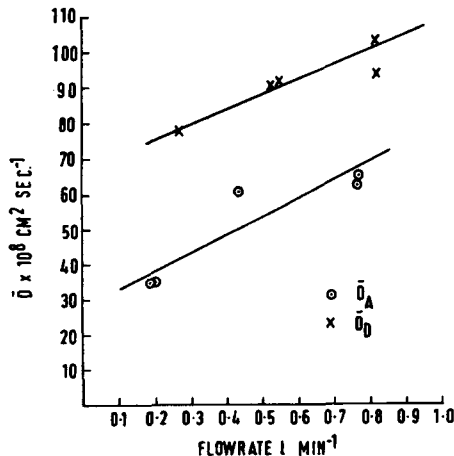


Fig. 3. Variation of \bar{D}_A and \bar{D}_D with flow rate of carrier gas at 60°C, 60% R.H. for S171.

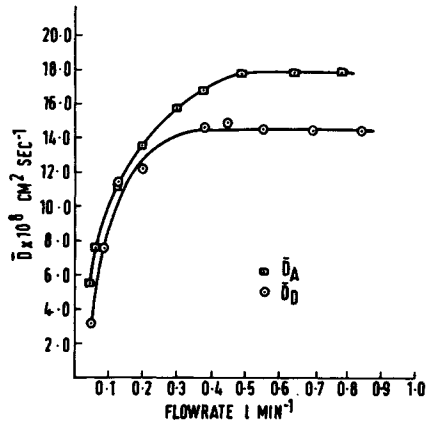


Fig. 4. Variation of \bar{D} with carrier gas flow rate at 60°C and 20% R.H. for S173.

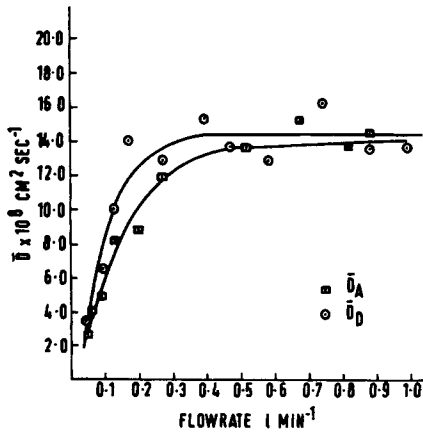


Fig. 5. Variation of \bar{D} with carrier gas flow rate at 60°C and 60% R.H. for S173.

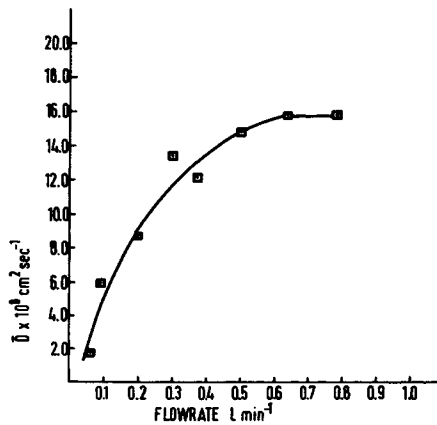


Fig. 6. Variation of \bar{D}_A with carrier gas flow rate at 60°C, 60% R.H. for S174.

Variation of the Measured Diffusion Coefficient with Flow Rate

All results showed a marked dependence of diffusion coefficient on flow rate. For the porous membrane S171 (Figs. 2 and 3), it continued to increase over the range of flow rates, whereas for the dense membranes S173 and S174 (Figs. 4, 5, and 6), it reached a limiting value at a flow rate of about 0.5 l/min.

To explain the results for the dense membranes, it is suggested that the carrier gas removes the heat of sorption by forced convection and that a balance between heat emission and removal is achieved at a critical flow rate.

The heat of sorption and associated temperature rise have been well documented.^{1,4,5} The increase in temperature due to the heat of sorption causes a decrease in the sorption rate because the surface concentration of water is decreased. This is due to the lowering of the thermodynamic activity at the constant vapor pressure and a higher temperature. The increase in temperature would also increase the diffusion coefficient, but it is expected that this effect will be small. Mathematically and experimentally, it has been shown⁵ that a sample is in equilibrium with the surrounding water vapor from very small times, less than 15 sec. This is achieved by a two-step mechanism. On initial sorption, the temperature rises abruptly and the thermodynamic activity of the water vapor falls to a value in equilibrium with the initial sorption. As the temperature falls, the equilibrium adjusts and the final regain is eventually approached. Cassie⁵ described results thus achieved as nothing more than cooling curves.

Heat may be lost from the sorption site in three ways: conduction into the sample, radiation, or convection from its surface. The second of these is a small effect and the third could not be used practically to achieve temperature control of samples before the advent of electrobalances, because of the instability of spiral springs in a flow system. The first method has been adopted so far to overcome the temperature problem, since by selecting thick enough samples it is possible to keep the temperature change to less than 1°C.

To explain the present results semiquantitatively, the heat removed by forced convection at various flow rates was calculated and compared with the heat evolved by the sorption process for membrane S174 at 60% R.H. The 45.0°C and 60°C isotherms for S174 (Fig. 7) provided the differential heat of sorption $\overline{\Delta H}_s$ (Fig. 8) using eq. (4):

$$-\overline{\Delta H}_s = \frac{2.303RT_1T_2}{(T_2 - T_1)} \log \frac{P_2}{P_1} \quad (4)$$

where P_1 is the equilibrium vapor pressure at temperature T_1 .

From the kinetic experiments, sorption-versus-time curves were obtained directly from the chart recorder, and it was thus possible to draw up a family of curves of % regain against time for different flow rates and hence produce another family of curves of heat of sorption against time (Fig. 9).

The rate of removal of heat by forced convection was calculated, using the following equations⁶:

$$\text{Re} = \frac{U_s \cdot x}{\nu} \quad (5)$$

where U_s = gas stream velocity, x = length of sheet, ν = kinematic viscosity, and Re = Reynold's number;

$$\text{Nu} = 0.331^3 \sqrt{\text{Pr}} \sqrt{\text{Re}} \quad (6)$$

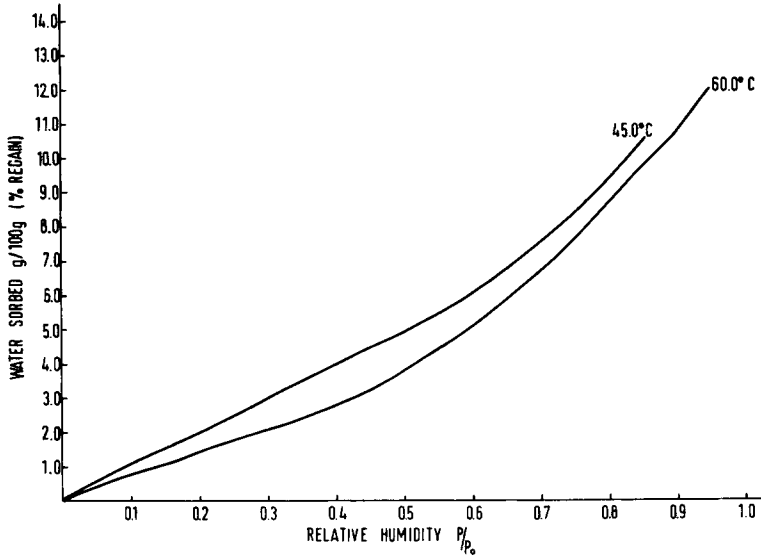


Fig. 7. Adsorption isotherms for S174 at 45.0°C and 60.0°C.

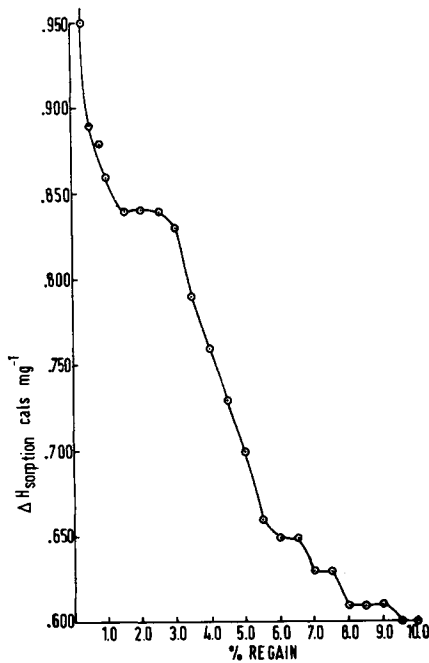


Fig. 8. Heat of sorption (45.0°C/60.0°C) vs. % regain for S174.

where Nu = Nusselt's number and Pr = Prandtl's number, obtained from tables;

$$h = \frac{k}{x} \cdot Nu \quad (7)$$

where k = thermal conductivity and h = local heat transfer coefficient;

$$h_m = 2h \quad (8)$$

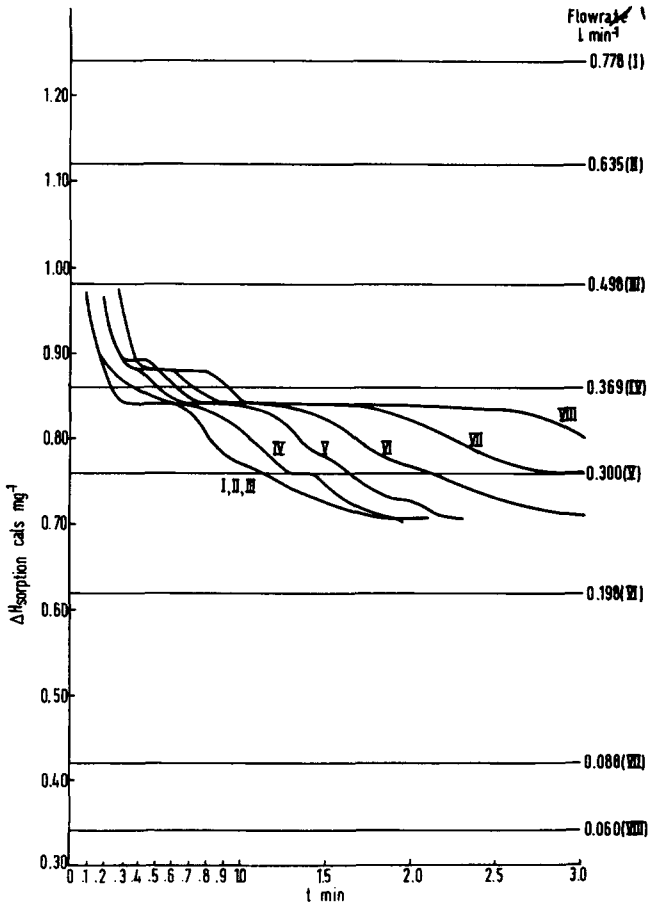


Fig. 9. Heat of sorption vs. time for various flow rates (S174 60°C, 60% R.H.). Horizontal lines represent forced convection at a given flow rate.

where h_m = overall heat transfer coefficient. Total heat removed from both sides is

$$Q = 2h_m b x \cdot \Delta T \quad (9)$$

where b = width of sheet and ΔT is the temperature difference between sample and carrier gas.

The following values⁶ were used in the calculation:

$$\nu \rho = 20 \times 10^{-5} \text{ ft}^2 \text{ sec}^{-1} \quad \text{Pr} = 0.68$$

$$k = 0.0186 \text{ Btu (hr)}^{-1} (\text{ft})^{-1} (^\circ\text{F})^{-1}.$$

This calculation contains two assumptions. The first is that there exists a temperature difference of 2°C between the sample and the carrier gas flowing past. This would be difficult to determine experimentally, but the very good agreement between calculated and experimental results would seem to justify the assumption. The second assumption may be more important. For the kinetic data, individual regains with time are not equilibrium sorption values, because only the sorption at infinite time, q_∞ , is made at equilibrium. Hence, when these

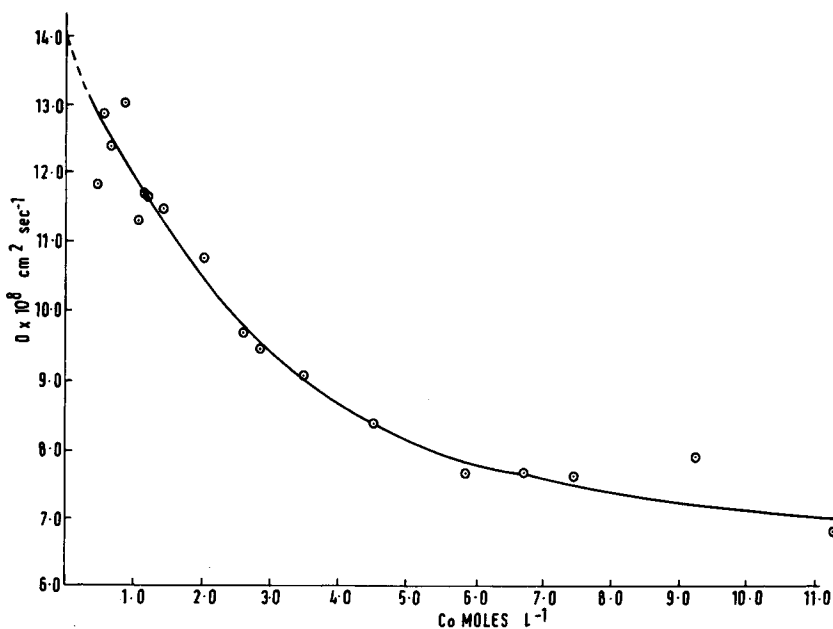


Fig. 10. Variation of diffusion coefficient D with equilibrium concentration C_0 for S174 at 60°C.

values are used to obtain the heat of sorption-versus-time curves, an error is introduced. Since heat of sorption decreases continually with time, however, the $\Delta\bar{H}_s$ values corresponding to the q_t values are greater than at equilibrium, and so in Figure 9 represent an upper limit. The lower limit will be provided by the heat of liquefaction of water which at the average temperature of 52.5°C is approximately 0.6 cal/mg. Hence, the calculation is certainly of the correct order.

Figure 9 also shows clearly the inadequacy of flow rates less than 0.369 l./min for maintaining constant sample temperature by forced convection and indicates the safety limit to be well in excess of 0.5 l./min. The spread of the curves clearly demonstrates the effectiveness of the forced convection at the various flow rates. The calculated results are in good agreement with those found experimentally for dense films.

Chabert et al.,⁷ using a gas-solid chromatographic technique to measure the diffusion coefficient of water in polyethylene glycol terephthalate fibrils, also observed the effect of gas flow rate on experimental results. The results in Figure 11 calculated from Chabert's data show that constant values of diffusion coefficient were obtained at flow rates in excess of 0.5 l./min, and in subsequent papers he has worked in excess of this flow rate, although no reason was given.

Three questions remain to be answered:

1. Why is there a discrepancy in Table I between some of the surface area determinations for water and nitrogen sorption? For S171 and S172, which are heterogeneous, porous membranes, the agreement is fairly good. However, as the membrane structure becomes finer, as in S170, less of the surface area is available to the nitrogen molecules, cross-sectional area 16.2 Å², whereas the water molecules with cross-sectional area 10.6 Å² are still able to penetrate most pores owing to swelling of the matrix. For the dense films S173 and S174, the majority

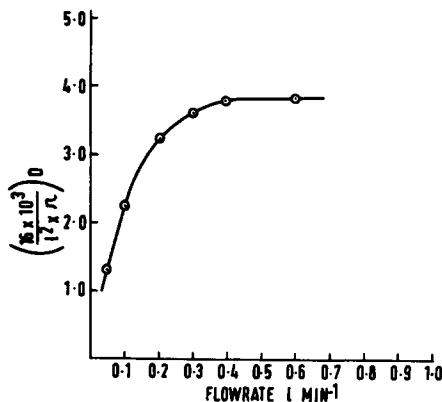


Fig. 11. Variation of diffusion coefficient with carrier gas flow rate (Chabert et al.⁷).

of the surface area is in small pores and hence produces the biggest divergence with the two adsorbates.

2. Why does the heterogeneous, porous membrane S171 show no limiting flow rate? Although B.E.T. water sorption data suggested similar surface areas for S171 and S173 (Table I), electron microscopy² shows that the pore structure is very different. S171 consists predominantly of large, open network pores while S173 and S174 have very small, closed pores. This means that the accessible surface area instantaneously available for water vapor sorption is larger in the case of the more open porous membrane. This would explain why for S171 the experimental \bar{D} values always depended on flow rate (Figs. 2 and 3), since forced convection is limited at the internal surface, where sorption takes place, and the resulting heat evolved will be conducted into the thin sample accompanied by a temperature rise.

3. We report a diffusion coefficient for water in cellulose acetate of 14.0×10^{-8} cm²/sec at 60°C compared with the value of $4-7 \times 10^{-8}$ cm²/sec found by others^{1,8} at that temperature. We suggest that this is because our casting dope contained formamide swelling agent, which was not used by the others, and that the inclusion opens up the structure of the system, providing a less tortuous path for diffusion.

The volume flow rates quoted in this paper are for our apparatus of rather irregular cross section (Fig. 1). Forced convection depends on linear gas velocity. For our apparatus, 0.5 l./min corresponds approximately to a linear gas velocity of 0.88 cm/sec (average cross-sectional area, 9.4 cm²).

Variation of Diffusion Coefficient with Concentration

This series of experiments was conducted for S174 at flow rates of 0.6 l./min to ensure comparable values for the integral diffusion coefficients. The diffusion coefficients were calculated using eq. (3) and were plotted against membrane concentration obtained from q_{∞} values (Fig. 10).

The decrease in diffusion coefficient is similar to that observed by Rouse,⁹ Barrer, et al.¹⁰ and many others,¹ and a discussion of this behavior is given by Barrie in reference 1. It has been suggested that clustering of water molecules, initiated by polar groups in the polymer, leads to immobilization of water and

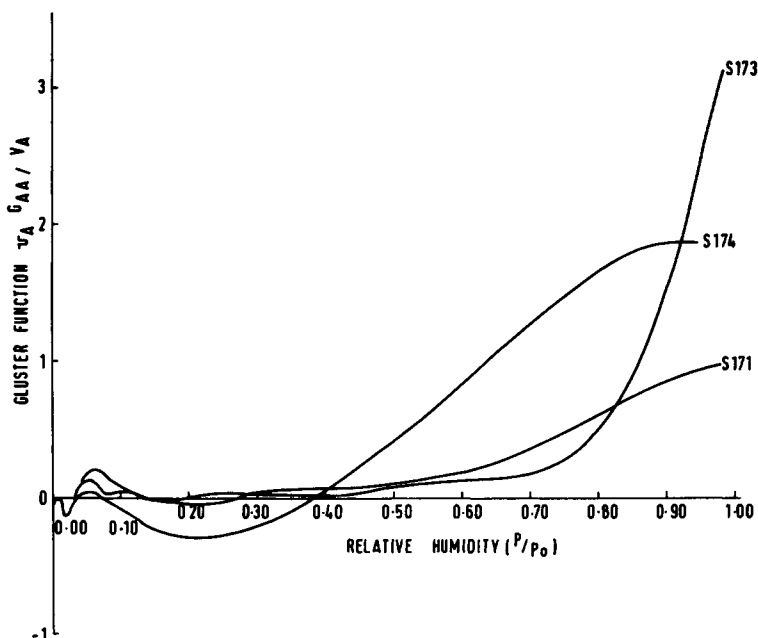


Fig. 12. Variation of cluster function with relative humidity for various membranes.

subsequent increase in the energy of activation for the diffusion process, due to the additional energy required to break up the clusters. Since clustering increases with increased concentration (Fig. 12), it is to be expected that diffusion coefficient would decrease with increased concentration. Cluster function curves in Figure 12 for S171, S173, and S174 were obtained by the method of Zimm and Lundberg¹¹ from sorption isotherm data. The higher the value of cluster functions, the more clustered the sorbed water. It can be seen that the dense membranes S173 and S174 show more clustering than the porous S171.

The dependence of diffusion coefficient on concentration for S171 can only be guessed at from our data, since limiting values could not be obtained. The values of \bar{D} at 60% R.H. are greater than at 20% R.H., suggesting an increase with concentration, as observed for cellulose by Newnes.¹² This may be due to a loosening of the structure of this open porous membrane as it is swollen by the sorbed water. The clustering of water molecules is less for this membrane (Fig. 12).

The variation of \bar{D}_A and \bar{D}_D with membrane and humidity is also notable (Figs. 2, 3, 4, and 5) since for the porous S171, $\bar{D}_A \simeq \bar{D}_D$ at 20% R.H. and $\bar{D}_A < \bar{D}_D$ at 60% R.H.; while for the dense S173, $\bar{D}_A > \bar{D}_D$ at 20% R.H. and $\bar{D}_A \simeq \bar{D}_D$ at 60% R.H. The relaxation of the polymer on desorption might explain $\bar{D}_D > \bar{D}_A$, but no reasonable explanation can be given for the reverse case observed in S173 (Fig. 4), although the absolute difference is very small. It seems that with the dense film, little swelling occurs compared with the more porous films.

Mr. M. J. Palin wishes to acknowledge the financial support of the Ministry of Defence and their permission to publish this paper. The authors are indebted to Mr. E. Goodinson for technical assistance and Professor R. F. Mann, R.M.C. Canada, for helpful discussions.

References

1. J. Crank and G. S. Park, *Diffusion in Polymers*, Academic Press, New York, 1968.
2. G. J. Gittens, P. A. Hitchcock, and G. E. Wakely, *Desalination*, **12**, 315 (1973).
3. B. C. Lippens, B. G. Linsen, and J. H. DeBoer, *J. Catalysis*, **3**, 32 (1964).
4. J. Crank, *The Mathematics of Diffusion*, Oxford University Press, Oxford, 1956.
5. G. King and A. B. D. Cassie, *Trans. Faraday Soc.*, **35-36**, 445 (1940).
6. E. R. G. Eckert, *Introduction to the Transfer of Heat and Mass*, McGraw-Hill, New York, 1950.
7. B. Chabert, J. Chauchard, and G. Edet, *C. R. Acad. Sci. Paris*, **271, Series C**, 38 (1970).
8. A. M. Thomas, *J. Appl. Chem. London*, **1**, 141 (1951).
9. P. Rouse, *J. Amer. Chem. Soc.*, **69**, 1068 (1947).
10. R. M. Barrer and J. A. Barrie, *J. Polym. Sci.*, **28**, 377 (1958).
11. B. H. Zimm and J. L. Lundberg, *J. Phys. Chem.*, **60**, 425 (1956).
12. A. C. Newnes, *Trans. Faraday Soc.*, **52**, 1533 (1956).

Received November 2, 1973

Revised June 28, 1974